applied optics

Evaluation of forward reflectance models and empirical algorithms for chlorophyll concentration of stratified waters

Zhongping Lee,[1,*] Yongchao Wang,[2] Xiaolong Yu,[2] Shaoling Shang,[2] and Kelly Luis[1]

[1]School for the Environment, University of Massachusetts Boston, Boston, Massachusetts 02125, USA
[2]State Key Laboratory of Marine Environmental Science, College of Ocean and Earth Sciences, Xiamen University, Xiamen 361102, China
*Corresponding author: zhongping.lee@umb.edu

Received 10 June 2020; revised 10 September 2020; accepted 10 September 2020; posted 11 September 2020 (Doc. ID 400070); published 14 October 2020

For waters with stratified chlorophyll concentration (Chl), numerical simulations were carried out to gain insight into the forward models of subsurface reflectance and empirical algorithms for Chl from the ocean color. It is found that the Gordon and Clark (1980) forward model for reflectance using an equivalent homogeneous water with a weighted average Chl ($\langle Chl \rangle$) as the input works well, but depending on the contribution of gelbstoff, the difference in reflectance between stratified and the equivalent homogeneous water can be more than 10%. Further, the attenuation of upward light is better approximated as ~1.5 times that of the diffuse attenuation coefficient of downwelling irradiance. On the other hand, although the forward model for reflectance developed in Zaneveld *et al.* [*Opt. Express* 13, 9052 (2005)] using equivalent homogeneous water with a weighted average of the backscattering to absorption ratio as the input also works well, this model cannot be used to obtain equivalent $\langle Chl \rangle$ for reflectance. Further, for empirical Chl algorithms designed for "Case 1" waters, it has been discovered that, for surface Chl in a range of ~0.06–22.0 mg/m^3, the predictability of surface Chl is basically the same as that of $\langle Chl \rangle$ from the blue-green band ratio or the band difference of reflectance. Because $\langle Chl \rangle$ is wavelength and weighting-formula dependent, and it is required to have profiles of both Chl and the optical properties, these results emphasize that for empirical Chl algorithms, it is easier, less ambiguous, and certainly more straightforward and simple to use surface Chl for algorithm development and then its evaluation, rather than to use $\langle Chl \rangle$, regardless of whether or not the water is stratified.

https://doi.org/10.1364/AO.400070

1. INTRODUCTION

There are many aspects in the study of ocean optics and ocean color remote sensing; these include (1) the modeling of the reflectance at sea surface using information of in-water constituents, or the forward model and (2) the estimation of in-water constituents from the reflectance, or the inverse model. A sound forward model is key to understanding the wide variety of observed color of natural waters, while inverse models are critical components to obtain the desired water properties from ocean color. For homogeneous waters, reflectance models have been developed for optically deep and shallow waters [1–7]; at the same time, a wide range of empirical or semi-analytical algorithms have been developed to retrieve water (and/or bottom) properties from a reflectance spectrum [8–14]. These models and algorithms have significantly advanced our understanding of the solar light in ocean as well as the spatial-temporal variations of phytoplankton in the global ocean and coastal environments [15–20].

Because of complex processes from solar radiation, nutrient supply, as well as mixing from various water masses, the upper water column is not always uniform [21,22]. Quite often there is a subsurface maximum of chlorophyll in oceanic waters [23], where the depth of this maximum (Z_{max}, m) could be a few meters to more than 100 m. The magnitude of concentration of chlorophyll (Chl, mg m^{-3}) at Z_{max} can be significantly larger than Chl near the surface. Depending on the overlaying optical properties, this layer of maximum Chl can have large contributions to the light measured by a remote sensor, and it thus stimulates questions on properly modeling the reflectance of stratified waters and accurately interpreting Chl estimated from an ocean color algorithm.

To address these questions, Gordon and Clark [24] were the first to propose the "concept of equivalence," where the

reflectance of stratified waters (R_s) is equivalent to that of a homogeneous water with a ratio ($\langle u \rangle$) of the backscattering (b_b) to the sum of b_b and absorption (a) coefficients. $\langle u \rangle$ is the weighted average of $b_b/(a+b_b)$ of the water column, where both a and b_b may vary with depth. For waters where phytoplankton is the main source of variation, Gordon and Clark [24] further suggested that R_s is equivalent to that of a homogeneous water with a chlorophyll concentration as $\langle \text{Chl} \rangle$, which is the weighted average of the stratified chlorophyll (Chl(z) hereafter). Further, it was suggested that this $\langle \text{Chl} \rangle$ could be used to compare with Chl empirically derived from reflectance (Chl^{RS}, hereafter) [24]. This concept of equivalence was further echoed in Gordon [25]. Later, Zaneveld *et al.* [26] developed a new framework for R_s from the radiative transfer equation (see more details in Section 2), where they obtained a theoretically different weighting formula from Gordon and Clark [24] and Gordon [25]. However, Zaneveld *et al.* [26] did not specify the details of calculating the weighting factors from different depths.

In the following years, many other studies assessed features of stratified waters, including the effect of Chl maximum on subsurface reflectance [27] and on the estimation of the photic depth [28], as well as algorithms for Chl of stratified waters [29,30]. However, few studies quantitatively evaluate the models for reflectance of stratified waters, especially regarding the required step to quantify the weighting factor. Also, few studies evaluated the applicability or necessity of $\langle \text{Chl} \rangle$ for empirical ocean color algorithms, which at present is the standard approach to process satellite ocean color measurements for Chl (https://oceancolor.gsfc.nasa.gov/). These limitations are described in details later after the various forward and inverse models are introduced in their complete forms.

In this study, after a brief review of the two forward models for reflectance, we use accurate simulations of stratified waters by Hydrolight [31] to quantitatively evaluate the forward models as well as to emphasize the ambiguities and challenges associated with $\langle \text{Chl} \rangle$ when empirical algorithms are used. Specifically, we first evaluate the schemes on the modeling of reflectance, as it is the core property to understand the variation of ocean color; second, we compare and evaluate the relationships between ocean color and the various Chl for empirical algorithms. The results of this effort provide new insights into the reflectance models of stratified waters and practical guidance to reduce ambiguities in remotely sensed Chl of stratified waters when empirical algorithms are chosen.

2. BRIEF REVIEW AND QUESTIONS OF THE REFLECTANCE MODELS PROPOSED FOR STRATIFIED WATERS

There are two forward models that were proposed in the past to analytically describe the subsurface reflectance of stratified waters; they are the model in Gordon and Clark [24] and that in Zaneveld *et al.* [26]. Other models, like the one in Sokoletsky and Yacobi [32], provided minor revisions of these two primary models by use of a different attenuation coefficient, with the essences of the two models remaining the same. Therefore, here we focus on the Gordon-Clark and Zaneveld models.

A. Gordon-Clark Model

For stratified waters, intuitively based on the round-trip attenuation of solar light before reaching a remote sensor that a reflectance is proportional to u [1–3], Gordon and Clark [24] and Gordon [25] suggested that R_s can be written as

$$R_s(\lambda) = R_b(\langle u(\lambda) \rangle_{\text{GC}}). \tag{1}$$

Here, R_b is the reflectance of an equivalent homogeneous water with a vertically weight-averaged $\langle u \rangle$ from the stratified water, and u is the ratio of b_b to the sum of b_b and a as follows:

$$u = \frac{b_b}{a + b_b}. \tag{2}$$

The subscript GC stands for the weighting scheme of Gordon and Clark [24], which is

$$\langle u(\lambda) \rangle_{\text{GC}} = \int_0^\infty u(z, \lambda) * W_{\text{GC}}(z, \lambda) \text{d}z, \tag{3}$$

where $W_{\text{GC}}(z, \lambda)$ is the weighting parameter for $u(z, \lambda)$ at a depth z written as follows:

$$W_{\text{GC}}(z, \lambda) = \frac{\exp(-2\tau(z, \lambda))}{\int_0^\infty \exp(-2\tau(z, \lambda)) \text{d}z}, \tag{4a}$$

with z (in m) downward from surface. Here, 2τ represents the round-trip optical distance of irradiance and is defined as

$$2\tau(z, \lambda) = \int_0^z (K_d(z', \lambda) + \kappa(z', \lambda)) \text{d}z', \tag{4b}$$

with

$$\int_0^\infty W_{\text{GC}}(z, \lambda) \text{d}z = 1. \tag{4c}$$

$K_d(z, \lambda)$ (in m^{-1}) in Eq. (4b) is the diffuse attenuation coefficient at wavelength λ of the downwelling irradiance, whereas $\kappa(z, \lambda)$ (in m^{-1}) is the attenuation coefficient for the light generated at z propagating upward [5,33], which is not the diffuse attenuation coefficient of the upwelling irradiance (K_u). As shown later, significant errors will be introduced to model R_s if κ is replaced by K_u. Gordon and Clark [24] and Gordon [25] indicated that it is effective to replace κ with K_d for the calculation of such a weighted average.

Originally, the integration of Eqs. (3)–(4) is from the surface to the penetration depth (Zp, m) [24], which is $1/K_d(\lambda)$ [34]. As Zp is wavelength dependent, and the contribution from Zp to infinite is just a few percent to the integration, so a truncation to Zp in Gordon and Clark [24] is appropriate. For easier description and consistency, we replaced Zp by ∞.

Because water's optical properties co-vary with Chl, Gordon and Clark [24] and Gordon [25] suggested to replace $u(z)$ in Eq. (3) by Chl(z), and obtained a weighted average of chlorophyll concentration ($\langle \text{Chl}(\lambda) \rangle$) as follows:

$$\langle \text{Chl}(\lambda) \rangle_{\text{GC}} = \int_0^\infty \text{Chl}(z) * W_{\text{GC}}(z, \lambda) \text{d}z. \tag{5}$$

Further, the reflectance of stratified water was proposed as [24,25]

$$R_s(\lambda) = R_b(\langle \mathrm{Chl}(\lambda)\rangle_{\mathrm{GC}}). \quad (6)$$

In short, when $\langle \mathrm{Chl}(\lambda)\rangle$ is available, it is perceived that R_s is equivalent to the reflectance of a homogeneous ocean having a chlorophyll concentration of $\langle \mathrm{Chl}(\lambda)\rangle_{\mathrm{GC}}$, under the assumption that the relationships of converting Chl to optical properties remain the same as that of the stratified water.

Using Monte Carlo simulations at 440 nm and 550 nm, Gordon [25] further showed that R_s based on Eqs. (4)–(6) has a maximum error below 2%–3% when both particle absorption ($a_p(z)$) and backscattering ($b_{\mathrm{bp}}(z)$) coefficients co-vary with Chl(z). If $b_{\mathrm{bp}}(z)$ is independent of Chl(z), however, there could be large errors when $\langle \mathrm{Chl}(\lambda)\rangle_{\mathrm{GC}}$ is used to estimate $R_s(\lambda)$.

B. Zaneveld Model

From the derivation of the radiative transfer equation, Zaneveld *et al.* [26] found that in principle, the average of u of the water column for reflectance can be expressed as follows:

$$\langle u(\lambda)\rangle_Z = \int_0^\infty u(z,\lambda) * W_Z(z,\lambda)\mathrm{d}z, \quad (7)$$

where the weighting function (termed as W_Z hereafter) is [32,35]

$$W_Z(z,\lambda) = \exp(-2\tau(z,\lambda))(K_d(z,\lambda) + \kappa(z,\lambda)). \quad (8)$$

Because reflectance is proportional to u [1,3], the average of Eq. (7) suggests that for stratified waters there is

$$R_s(\lambda) = R_b(\langle u(\lambda)\rangle_Z). \quad (9)$$

By comparing Eqs. (7)–(9) with Eqs. (1)–(3), one can find that the overall concept between R_s and $\langle u\rangle$ is the same between the two forward models, but the weighting function is very different, thus $\langle u\rangle$ from the two models will be different for the same stratified waters, so do the resulted R_s.

C. Further Questions of These Forward Models

Because Eqs. (7)–(8) are derived from radiative transfer equation, it was suggested in Zaneveld *et al.* [26] that the weighting scheme could be applicable to other remote sensing parameters, such as $\langle \mathrm{Chl}\rangle$. Thus, $\langle \mathrm{Chl}\rangle$ could be written as follows:

$$\langle \mathrm{Chl}(\lambda)\rangle_Z = \int_0^\infty \mathrm{Chl}(z) * W_Z(z,\lambda)\mathrm{d}z. \quad (10)$$

However, it is not known if, even for waters where the vertical profiles of inherent optical properties (IOPs) co-vary with Chl(z), a prerequisite emphasized in Zaneveld *et al.* [26], will the following relationship be true:

$$R_s(\lambda) = R_b(\langle \mathrm{Chl}(\lambda)\rangle_Z)? \quad (11)$$

Further, although $a_p(z)$ and $b_{\mathrm{bp}}(z)$ co-vary with Chl(z) in the Monte Carlo simulations of Gordon [25], the absorption of gelbstoff (a_g) was excluded in the simulations, thus the conclusion of "maximum 2%–3% error" of a model like Eq. (6) may be limited to such special cases. As a_g increases exponentially with a decrease of wavelength, a_g could be a significant contributor to $2\tau(\lambda)$ at least in the shorter wavelengths. It is thus necessary to know the potential effect of a_g on a model like Eq. (6), even if both $a(z)$ and $b_b(z)$ are still kept to co-vary with Chl(z).

Furthermore, although a conceptual relationship between R_s and $\langle u\rangle$ is provided in Zaneveld *et al.* [26], the way to quantify the weighting parameter required to obtain the average is not specified. On the other hand, the assumption of $\kappa = K_d$ in Gordon and Clark [24] is intuitive; it is not derived from the radiative transfer equation. It was suggested in Sathyendranath and Platt [5] that κ could be much larger than K_d. In a study through Monte Carlo simulations, Piskozub *et al.* [36] tested the model performances in two cases (bubble layer and high chlorophyll layer) by assuming $\kappa = K_u$, a/μ_d, and $(a + b_b)/\mu_d$, respectively, with μ_d being the average cosine of the downwelling light field [37]. Piskozub *et al.* [36] obtained a good closure (~1% difference) with $\kappa = K_u$. However, as shown later, the use of K_u to replace κ introduced large errors in the modeling of reflectance. Although μ_d is not always available in field measurements, the specification of κ for the calculation of the weighted averages is still not clear. Following the intuitive assumption of $\kappa = K_d$ in Gordon and Clark [24] and Gordon [25], a more general assumption between κ and K_d could be

$$\kappa(z,\lambda) = \gamma * K_d(z,\lambda). \quad (12)$$

Then a question arises: what is a more appropriate value for γ when calculating the various weighted averages?

3. EVALUATION OF THE FORWARD REFLECTANCE MODEL OF STRATIFIED WATERS

A. Numerical Simulations

To answer the above questions, as in Stramska and Stramski [27], Hydrolight [31] was used to simulate the subsurface light field for stratified and equivalent homogeneous waters where Chl is the input parameter for reflectance. Since Gordon [25] and Zaneveld *et al.* [26] numerically and theoretically demonstrated that the previously mentioned forward models will not work with $\langle \mathrm{Chl}\rangle$ if $b_{\mathrm{bp}}(z)$ does not co-vary with Chl(z), here the numerical simulations focused on scenarios that both $a_p(z)$ and $b_{\mathrm{bp}}(z)$ co-vary with Chl(z), but the vertical variation of $a_g(z)$ is treated differently. Nevertheless, the resulting $a(\lambda)$ still co-varies with Chl(z), as shown in Fig. 1 for an example.

Following Stramska and Stramski [27], the vertical distribution of Chl is parameterized as [21,22,38]

$$\mathrm{Chl}(z) = C_0 + C_m \exp\left(-\frac{(z - Z_{\max})^2}{\sigma^2}\right), \quad (13)$$

where C_0 is the background Chl, C_m determines the amplitude of the chlorophyll maximum, $Z_{\max}$ is the depth of deep chlorophyll maximum (DCM), and σ reflects the vertical thickness of the chlorophyll maximum layer. To enhance the contribution of the DCM layer to subsurface reflectance, we set $C_0 = 0.05\ \mathrm{mg\ m^{-3}}$, $Z_{\max} = 10\ \mathrm{m}$, $C_m = 5\ \mathrm{mg\ m^{-3}}$, and $\sigma = 3\ \mathrm{m}$; this is a profile similar to that in Piskozub *et al.* [36]. Further, the following three cases were designed to have different contributions of a_g, which are, in general, in the ranges observed in natural environments.

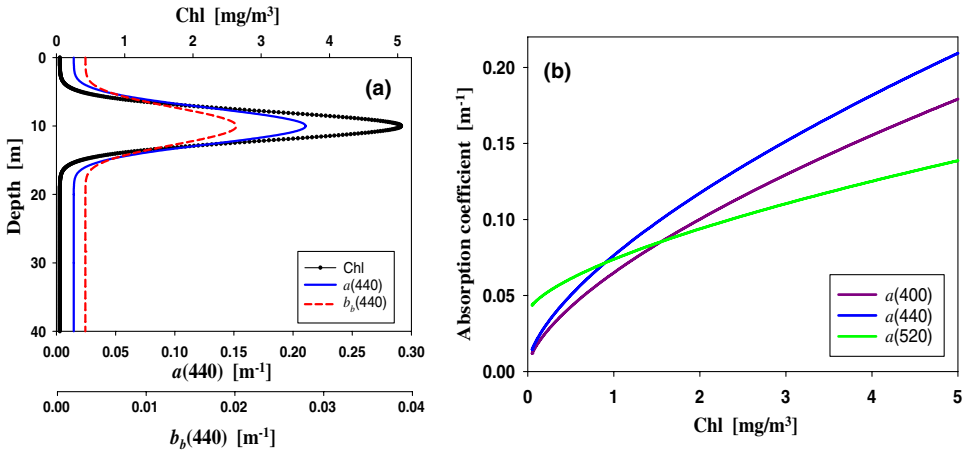

Fig. 1. (a) Profiles of Chl(z) and optical properties; (b) relationship between Chl and the absorption coefficient.

Case #1: $a_g(z, 440) = 0.2{*}a_p(z, 440)$.
Case #2: $a_g(z, 440) = 2{*}a_p(z, 440)$.
Case #3: $a_g(z, 440) = 0.1\ \mathrm{m}^{-1}$ and independent of depth.

Therefore, for each case, the total absorption co-varies with Chl(z) (see Fig. 1). The vertical resolution employed in Hydrolight simulations is 0.05 m to ensure the precision for numerical integration over the weighting parameters. This was tested by checking the value from Eq. (4c), where this integration is around or greater than 0.98 for all wavelengths. Piskozub *et al.* [36] used a vertical resolution of 2 m in their Monte Carlo simulations, which may not have sufficient precision to address the modeling of stratified waters.

It is also required to convert Chl(z) to a_p and b_{bp} in Hydrolight simulations. For the three cases listed previously, the same bio-optical conversion models and parameters embedded in Hydrolight were used for all depths; therefore, the resulting $a_p(z)$ and $b_{\mathrm{bp}}(z)$ co-vary with Chl(z). As there are many articles describing the numerical simulations using Hydrolight [7,27,39,40]; some of the details of the bio-optical models used in this study are summarized in A. The wavelengths for this study are 360, 400, 440, 480, 520, 560, 600, and 640 nm, as shorter or longer wavelengths have short penetration depth [34], where the effect of DCM is small or negligible. Figure 1 shows the Chl(z) profile and the co-variance between the bulk absorption coefficient and Chl for Case #1.

B. Comparison of ⟨Chl⟩ With Different κ (or γ)

We first compared the weight-averaged $\langle \mathrm{Chl} \rangle_{\mathrm{GC}}$ where different values of γ in Eq. (12) were used to estimate κ, with results showing in Figs. 2(a)–2(c) for the three designed cases. Here, three γ values were used, which are 1.0, 1.5, and 2.0, with $\langle \mathrm{Chl} \rangle_{\mathrm{GC-1.0}}$, $\langle \mathrm{Chl} \rangle_{\mathrm{GC-1.5}}$, and $\langle \mathrm{Chl} \rangle_{\mathrm{GC-2.0}}$ representing the resulting corresponding averages, respectively. Note that the default γ value in Gordon and Clark [24] and Gordon [25] is 1.0. Also included in Fig. 2 is Zp [34] of the three cases, which is generally ~9 m for the ~450−550 nm range, but it is ~3 m at 640 nm. As Z_{max} is 10 m, these Zp values indicate that reflectance for wavelengths around 450–550 nm will include strong contributions from the layer of maximum Chl, but reflectance at 640 nm will not.

Since ⟨Chl(λ)⟩ is a light-weighted average, ⟨Chl(λ)⟩ will be wavelength dependent, as represented by Eq. (5) and showing in Fig. 2. In view of this basic nature, any ⟨Chl⟩ calculated from the use of the diffuse attenuation coefficient of photosynthetic available radiation (Kpar, m^{-1}) [22,32] will not be appropriate to model $R_s(\lambda)$, as Kpar is not wavelength resolved, whereas $R_s(\lambda)$ is. More importantly, it appears that a change of γ can have a significant effect on ⟨Chl(λ)⟩, at least for the stratified cases here. For instance, when γ value was changed from 1.0 to 1.5, $\langle \mathrm{Chl}(\lambda) \rangle_{\mathrm{GC}}$ decreased by about 15%–36% for Cases #1–3, and this decrease is about 28%–52% for the three cases when γ value is changed from 1.0 to 2.0. This is because when γ increases, the round-trip attenuation also increases; thus Chl(z) at deeper depths has relatively less weighting in ⟨Chl(λ)⟩. At the same time, Chl(z) is lower near the surface (see Fig. 1), so a smaller ⟨Chl(λ)⟩ will result when γ value increases. These results highlight the necessity to determine a more appropriate γ value for the weighted averages, as different ⟨Chl(λ)⟩ will result in different $R_s(\lambda)$ from the forward model based on Eq. (5) (also see below).

As hinted in Zaneveld *et al.* [26], ⟨Chl⟩ of Case #1 calculated following the weighting formula of Eq. (10) ($\langle \mathrm{Chl} \rangle_Z$) are presented in Fig. 2(d) for a comparison, which shows that, as a result of the different weighting formula, $\langle \mathrm{Chl} \rangle_Z$ is about two times that of $\langle \mathrm{Chl} \rangle_{\mathrm{GC}}$ for each γ value. As shown later in this article and expected, this has significant consequences on the modeling of R_s following the concept of equivalent homogeneous waters with ⟨Chl⟩ as the concentration of chlorophyll.

C. Comparison of the Forward Models Using ⟨Chl(λ)⟩ as the Input

Because a remote sensor measures radiance or remote sensing reflectance, here, for the three cases, we compared subsurface remote sensing reflectance (r_{rs}) of stratified waters with that estimated by Eq. (6). r_{rs} (nadir viewing here) is defined as the ratio of upwelling radiance to downwelling irradiance measured just below the surface. Figure 3 shows the relative difference (RD) of r_{rs}, calculated as

$$\mathrm{RD}(\lambda) = \frac{r_{\mathrm{rs}}^{\mathrm{eh}}(\lambda) - r_{\mathrm{rs}}^{\mathrm{stra}}(\lambda)}{r_{\mathrm{rs}}^{\mathrm{stra}}(\lambda)}. \tag{14}$$

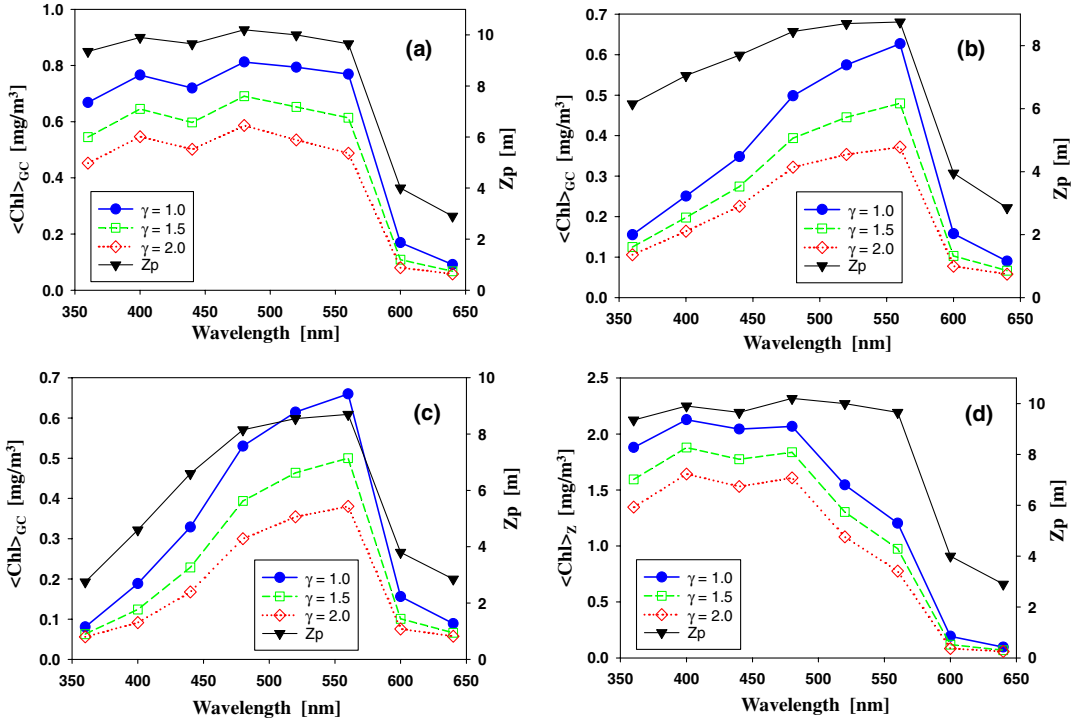

Fig. 2. Weighted average of Chl with different treatment of κ and model for the weighting factor. (a)–(c) for the three cases based on the weighting formula of Gordon and Clark [24]; (d) for Case #1 based on the weighting formula of Zaneveld *et al.* [26].

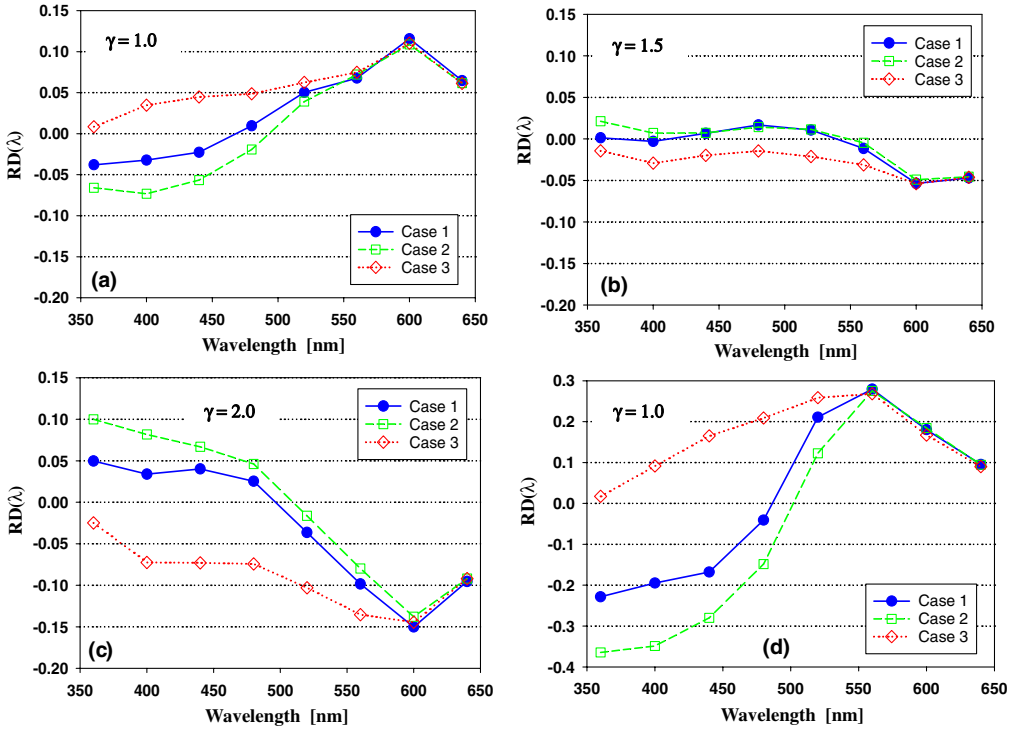

Fig. 3. Error of modeled r_{rs} with the concept of equivalent homogeneous using ⟨Chl⟩ as the input. (a)–(c) for the three cases where ⟨Chl⟩ was calculated based on the weighting formula of Gordon and Clark [24], but different γ values; (d) $\gamma = 1.0$, but ⟨Chl⟩ was calculated using the weighting formula of Zaneveld *et al.* [26].

Here, superscript "stra" represents r_{rs} obtained from Hydrolight simulations of stratified waters, whereas the superscript "eh" represents r_{rs} also simulated by Hydrolight, but for an equivalent homogeneous water body with a Chl of ⟨Chl(λ)⟩. The bio-optical conversions were kept the same for both Hydrolight simulations.

For the three cases discussed here, it is found that [see Fig. 3(a)] when $\langle \mathrm{Chl}(\lambda)\rangle_{\mathrm{GC}-1.0}$ was used to model r_{rs} following Eq. (6), RD(λ) is in a range of ∼−7.3% to 11.3% for wavelengths of 360–640 nm. RD(λ) can differ substantially between wavelengths and between the different IOPs-Chl setups, although for each case, $a(z,\lambda)$ and $b_b(,z,\lambda)$ co-vary with Chl(z). For example, when $\gamma = 1.0$ was used, RD(λ) is negative (lower r_{rs} from ⟨Chl⟩) for the 360–500 nm range for Case #2, but RD(λ) becomes positive (higher r_{rs} from ⟨Chl⟩) for Case #3. Further, RD(λ) is more negative for Case #2 than for Case #1, where there are more contributions from a_g to the total absorption coefficient. However, the previously mentioned patterns are reversed for $\gamma = 2.0$ [see Figs. 3(a) and 3(c)]. These results echo the complexity in modeling the reflectance of stratified waters [26].

More importantly, these values are much higher than the "maximum error ∼2−3%" presented in Gordon [25] for wavelengths at 440 nm and 550 nm, indicating the effect of a_g on the concept of equivalent homogeneous water, where a_g was excluded in Gordon [25]. This is because for the same profiles of Chl(z), when $a_g(z,\lambda)$ is added, it will effect $2\tau(z,\lambda)$ and subsequently $\langle \mathrm{Chl}(\lambda)\rangle$ following Eq. (5). Further, $r_{\mathrm{rs}}(\lambda)$ is not a linear function of $a(\lambda)$, nor is $\langle \mathrm{Chl}(\lambda)\rangle$ a linear function of $a_g(\lambda)$. Therefore, greater differences are found in RD(λ) for wavelengths in the 360–560 nm range.

On the other hand, it is interesting that when $\langle \mathrm{Chl}\rangle_{\mathrm{GC}-1.5}$ is used to model r_{rs} following Eq. (6), RD(λ) is reduced to a range of ∼−5% to 2% for wavelengths of 360–640 nm [see Fig. 3(b)]. Further, if $\langle \mathrm{Chl}\rangle_{\mathrm{GC}-2.0}$ is used to model r_{rs} following Eq. (5), RD(λ) is in a range of ∼−15% to 10% for the same wavelength range [(Fig. 3(c)]. These results suggest that, at least for the simulated cases here, a γ value of ∼1.5 rather than 1.0 appeared more appropriate for the calculation of ⟨Chl⟩ of stratified waters following the concept of equivalent homogeneous.

Although it is tempting to determine an optimal γ value for all stratified waters, simulating the enormous possible scenarios of stratifications is beyond the scope of this work. The results rather indicate that even for IOPs(z, λ) that co-vary with Chl(z), the error of modeling $r_{\mathrm{rs}}(\lambda)$ of stratified waters based on equivalent homogeneous water with ⟨Chl⟩ as the input could be much larger than 2%–3%, especially if a default γ of 1.0 is used.

r_{rs} of equivalent homogeneous water with $\langle \mathrm{Chl}\rangle_{Z-1.0}$ of the three cases was also simulated by Hydrolight and compared with that of stratified waters, with the resultant RD(λ) shown in Fig. 3(d) for a comparison. It is found that the values of RD(λ) are in a range from −36.5% to 27.5% for the 360–640 nm range of the three cases, indicating much worse performance in modeling r_{rs} using $\langle \mathrm{Chl}\rangle_{Z-1.0}$, although the IOPs($z$) co-vary with Chl($z$) for each case and each wavelength. This is due to the fact that the weighting function of Zaneveld *et al.* [26] is also linearly dependent on the attenuation coefficient [see Eq. (8)], where the contributions of both a_g and b_{bp} (which are part of K_d) would be converted to $\langle \mathrm{Chl}\rangle_{Z-1.0}$, which is then much larger than $\langle \mathrm{Chl}\rangle_{\mathrm{GC}-1.0}$ [see Fig. 2(d)]. These results suggest that, although Eq. (7) was derived from the radiative transfer equation, it is strictly for ⟨u⟩, a ratio associated with b_b and a, not for ⟨Chl⟩ if a closure is desired between the R_s and $R_b(\langle \mathrm{Chl}\rangle)$.

D. Comparison of the Forward Models Using ⟨u⟩ as the Input

Reflectance is a function of u in general [1,3,5], and two different weighting schemes [Eq. (3) and Eq. (7)] were proposed to obtain the ⟨u⟩ of stratified waters for reflectance. Because of the difference in physics and mathematics formulas, these two weighting models will result in different ⟨u⟩ and then different reflectance for the same stratified water body. Through Monte Carlo simulations with subsurface Chl maximum in the 10–20 m layer, Piskozub *et al.* [36] showed that Eq. (7) can, in general, obtain reasonable reflectance, not Eq. (3). However, as shown previously regarding ⟨Chl⟩, the calculation of ⟨u⟩ is dependent on the treatment of κ, where Piskozub *et al.* [36] obtained the conclusions by taking $\kappa = K_u$, which is not supported by the theory of radiative transfer [5,33]. Since the weighting formula for ⟨u⟩ in Gordon and Clark [24] is not supported from the radiative transfer equation for stratified waters, we evaluated r_{rs} with the ⟨u⟩ formula of Zaneveld *et al.* [26] only, with γ value also as 1.0, 1.5, and 2.0, respectively. Further, since a Hydrolight simulation requires inputs of absorption and scattering properties, not the ratio of $b_b/(a+b_b)$ and the reflectance model of homogeneous waters is well developed [1–7], r_{rs} for each ⟨u⟩ is calculated following the model of Gordon *et al.* [3]:

$$r_{\mathrm{rs}}(\lambda) = (0.0979 + 0.0794\langle u(\lambda)\rangle)\langle u(\lambda)\rangle. \tag{15}$$

This modeled r_{rs} is then compared with r_{rs} obtained from the Hydrolight simulations of stratified waters, with RD(λ) calculated following Eq. (14) for the three γ values and shown in Figs. 4(a)–(c). For a γ of 1.0 [Fig. 4(a)], RD(λ) is in a range about −8.0% to 6.0%, but it becomes −12% to 12% for a γ of 1.5 and −22% to 18% for a γ of 2.0. These results suggest that, unlike a γ value of 1.5 used for ⟨Chl⟩ to obtain a more consistent reflectance, a γ value of 1.0 works better for ⟨u⟩ to model r_{rs}. The non-zero RD(λ) and its dependence on wavelength and IOPs further show the complexity of modeling r_{rs} of stratified waters. Also note that the modeling coefficients (0.0979, 0.0794) are kept as constants vertically; as pointed out in Zaneveld *et al.* [26], these modeling coefficients could also vary with depth, as the radiance distribution is a function of depth [37].

As in Piskozub *et al.* [36], we tested using K_u to replace κ in Eq. (8) for calculating the weighting parameter, and the resultant RD(λ) is shown in Fig. 4(d). These values are significantly larger (as high as 80%) than those using the three γ values to estimate κ following Eq. (12). This result is contradictory to the findings of Piskozub *et al.* [36], where they found a difference of less than 1%. It is necessary to emphasize that theoretically, because κ is not K_u and K_u is larger than K_d [5], replacing κ with K_u is not expected to obtain such a small difference in modeling reflectance following Eqs. (7)–(8) and (15).

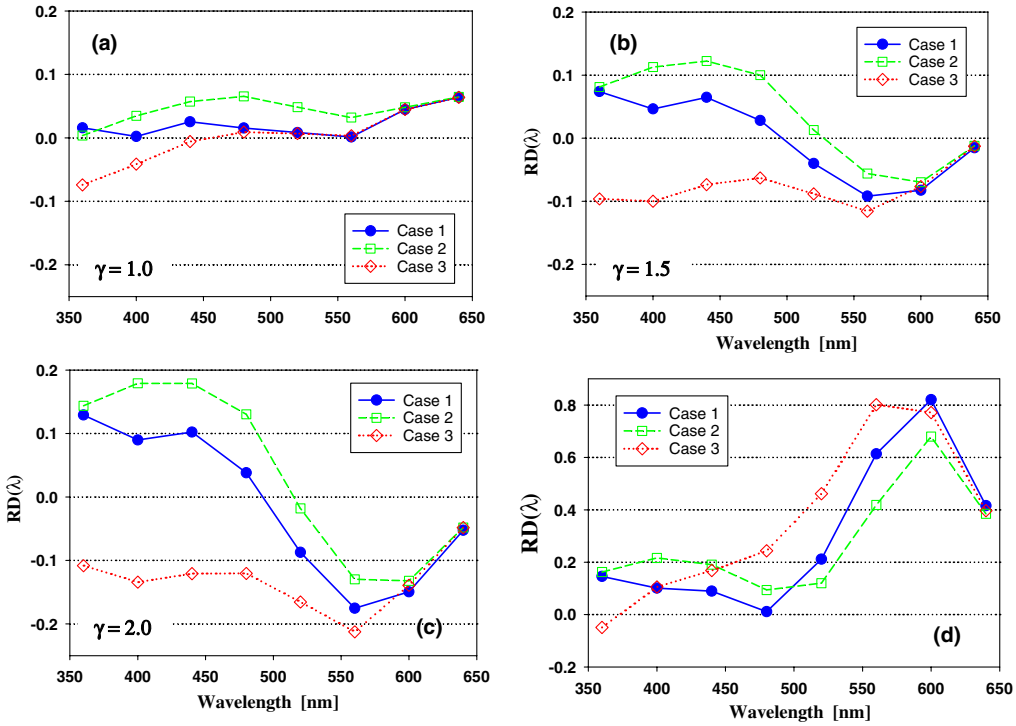

Fig. 4. Error of modeled r_{rs} with the concept of equivalent homogeneous using as the input. (a)–(c) for the three cases where u was calculated using the weighting formula of Zaneveld *et al.* [26], but different γ values; (d) was calculated as (a)–(c), but assumed $\kappa = K_u$ as in Piskozub *et al.* [36].

4. EMPIRICAL ALGORITHM FOR CHL OF STRATIFIED WATER

A. Brief Overview of Empirical Algorithm for and Challenge of the Chl of Stratified Waters

Presently, Chl products from ocean color satellites are generally produced using empirical algorithms, with band ratios [8] or band differences [11] of R_{rs} as the input, such as the common OC4 algorithm adopted by National Aeronautics and Space Administration (NASA):

$$\mathrm{Chl}^{\mathrm{RS}} = 10^{\alpha_0+\alpha_1\times \mathrm{RR}+\alpha_2\times \mathrm{RR}^2+\alpha_3\times \mathrm{RR}^3+\alpha_4\times \mathrm{RR}^4} \tag{16a}$$

and

$$\mathrm{RR} = \log_{10}\left(\frac{\mathrm{Max}(R_{rs}(\lambda_1),\ R_{rs}(\lambda_2),\ R_{rs}(\lambda_3))}{R_{rs}(\lambda_4)}\right). \tag{16b}$$

Here, R_{rs} is the above-surface remote sensing reflectance, which can be converted from r_{rs} [3,41]. $\lambda_{1\sim3}$ are wavelengths in the range between 440 and 510 nm, and λ_4 is around 550 nm. $\alpha_{0\sim4}$ are empirical coefficients derived by pooling global measurements [8]. For Chl $<\sim 0.25$ mg m^{-3}, an empirical algorithm based on differences of R_{rs} is employed [11]:

$$\mathrm{Chl}^{\mathrm{RS}} = 10^{\beta_0+\beta_1\times \mathrm{CI}}[\mathrm{CI} < -0.0005\ \mathrm{sr}^{-1}] \tag{17a}$$

and

$$\mathrm{CI} = R_{rs}(555) - \left[R_{rs}(443) + \frac{555-443}{670-443} * (R_{rs}(670) - R_{rs}(443))\right], \tag{17b}$$

with β_0 and β_1 the empirical coefficients.

For homogeneous waters, $\mathrm{Chl}^{\mathrm{RS}}$ obtained from Eqs. (16) or (17) can be directly compared with Chl measured at a depth to evaluate the performance of such algorithms. For stratified waters, because $R_{rs}(\lambda)$ has information of Chl(z) from the upper water column, it was then argued that this $\mathrm{Chl}^{\mathrm{RS}}$ should be compared with $\langle \mathrm{Chl}\rangle_{\mathrm{GC}}$ calculated via Eq. (5). Although this concept of using the weighted average for remotely sensed Chl or IOPs has been followed in the past decades [42–46], there is no consensus on which $\langle \mathrm{Chl}\rangle$ should be used to compare with $\mathrm{Chl}^{\mathrm{RS}}$ [22,32,44,47,48]. This is because, as shown in the literature [25] and Fig. 2, 2τ is wavelength dependent, and the resultant $\langle \mathrm{Chl}\rangle$ is a wavelength- and formula-dependent product. It is quite a dilemma and challenge to ensure consistent and appropriate $\langle \mathrm{Chl}\rangle$ for the evaluation of $\mathrm{Chl}^{\mathrm{RS}}$ [28,47].

Using numerically simulated data, Andre [47] compared $\langle \mathrm{Chl}(520)\rangle_{\mathrm{GC-1.0}}$ with $\mathrm{Chl}^{\mathrm{RS}}$ derived from a 443–550 band ratio algorithm [43], and concluded that only for strong stratifications happening near the surface, this weighted average is necessary. Andre [47] argued that for a majority of the ocean, it is not required to calculate $\langle \mathrm{Chl}\rangle$ for the evaluation of $\mathrm{Chl}^{\mathrm{RS}}$, in particular, given the complexity and the requirement of optical data associated with the calculation of $\langle \mathrm{Chl}\rangle$. However, Andre's analysis [47] only used chlorophyll information at 520 nm ($\langle \mathrm{Chl}(520)\rangle_{\mathrm{GC-1.0}}$), the simulated dataset used had relatively mild stratifications, and $\mathrm{Chl}^{\mathrm{RS}}$ was derived from an algorithm for homogenous waters. In view of the refinement and advancement of empirical algorithms for Chl from ocean color satellites [8,11], we extended this analysis to other wavelengths along with much stronger stratification of Chl

(in addition to an accurate simulation of reflectance of stratified waters by Hydrolight). The objective is to emphasize that it is not a must to calculate ⟨Chl⟩ for stratified waters when empirical algorithms are the route for Chl^{RS}. This is also because, if ⟨Chl⟩ is to be used for the evaluation of Chl^{RS} derived from algorithms like Eqs. (16) or (17), the algorithm coefficients ($\alpha_{0\sim4}$ or β_{0-1}) should first be derived using the same type of ⟨Chl⟩, which is not the case presently or that in Andre [47]. Also, note that there is no requirement of closure between the input R_{rs} (or r_{rs}) and the R_{rs} modeled using the Chl obtained from Eqs. (16) or (17) in such applications of ocean color remote sensing. Therefore, ⟨Chl(Kpar)⟩ as in Morel and Berthon [22] and Sokoletsky and Yacobi [32] is applicable if necessary.

B. Data of Stratified Waters for Empirical Chl Algorithm

To demonstrate why ⟨Chl⟩ of stratified waters is not a must for empirical algorithms, as earlier studies and the evaluation of the forward model for reflectance, numerical simulations with Hydrolight were carried out to generate a dataset having a wide range of Chl(z) and its corresponding R_{rs}. This dataset has Chl in the surface layer varied from ∼0.06 to 22.0 mg m^{-3}. The range of Chl is divided into 1000 levels with an equal interval in log scale, thus having a balanced distribution from the low to high end. Since the empirical algorithms are designed for "Case 1" waters [49] only, IOPs(z) of other water constituents (except the contributions of water molecules) are all determined by Chl(z).

Profiles of vertical Chl(z) were also modeled based on Eq. (13). Following Morel and Berthon [22], the four variables (C_0, C_m, Z_{max}, and σ) in Eq. (13) were designed to co-vary with a free variable (C hereafter), and the relationships are as follows:

$$C_0 = 0.23\exp(1.45 * \mathrm{Log}(C)), \quad \textbf{(18a)}$$

$$C_m = 5 * \exp(1.3 * \mathrm{Log}(C)), \quad \textbf{(18b)}$$

$$Z_{max} = 6.9*(\mathrm{Log}(C))^2 - 30.23 * \mathrm{Log}(C) + 30.9, \quad \textbf{(18c)}$$

and

$$\sigma = 8.15*(\mathrm{Log}(C))^2 - 16.07 * \mathrm{Log}(C) + 13.19. \quad \textbf{(18d)}$$

The range of C is 0.02−20.0 mg m^{-3}, whereas the coefficients in the relationships were adjusted slightly from those in Morel and Berthon [22] to ensure an adequate effect of the DCM layer on R_{rs}. From such a setup, the range of C_0 is about 0.02−1.5 mg m^{-3}, C_m about 0.5−27.1 mg m^{-3}, Z_{max} is in a range of 3.2–102 m (deeper for clear waters), and surface Chl (Chl(0)) varied from ∼0.06−22.0 mg m^{-3}. Note that intentionally here the synthesized Chl(z) increases much faster than the *in situ* profiles used in Andre [47], as indicated in the large ratios of ⟨Chl⟩/Chl(0.5) (see Fig. 5). Also, differing from Andre [47] who used an approximation to obtain subsurface reflectance, here an accurate numerical model (Hydrolight [31]) is employed to simulate in-water light field and R_{rs}. In the simulations, the water column is set as infinitely deep with the calculation stopped at 120 m, and no Raman scattering or fluorescence is included. The sky is set as cloudless with a sun zenith angle of 30°, and a wind speed of 5 m s^{-1} is used.

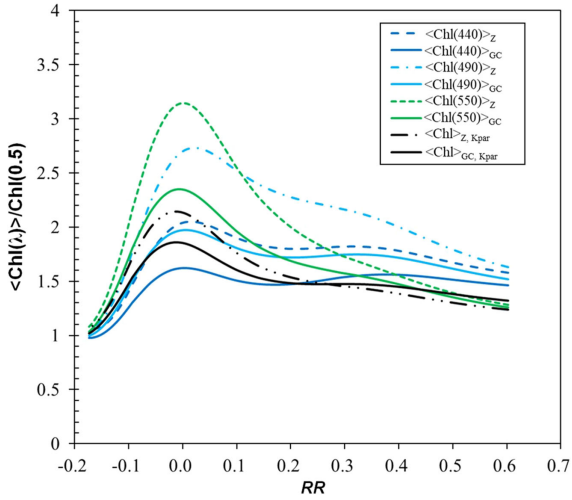

Fig. 5. Ratio of ⟨Chl⟩ to Chl(0.5) for 1000 cases of stratified waters, where Chl(0.5) varied from ∼0.06−22.0 mg/m^3, and ⟨Chl⟩ were calculated for different wavelengths and formulae.

C. Relationships Between Chl^{RS} and ⟨Chl⟩ as Well as Chl(0.5)

1. Variations of Weighted Average of Chlorophyll Profile

To further echo the wavelength and formula dependence of ⟨Chl⟩, the ratios of various ⟨Chl⟩ to Chl(0.5) are presented in Fig. 5. Chl(0.5) here is selected to represent Chl of the "surface" layer; certainly, Chl from another depth near the surface or an arithmetic average of the near-surface layer [32] could also serve this purpose. For all calculations of ⟨Chl⟩, a γ value of 1.0 was used here. It is found that the ratio of $\langle Chl(440)\rangle_{GC}$ to Chl(0.5) is in a range of ∼0.9−1.6, whereas it is ∼1.0−2.3 for $\langle Chl(550)\rangle_{GC}$ to Chl(0.5), and ∼1.0−1.7 for $\langle Chl(Kpar)\rangle_{GC}$ to Chl(0.5). Also, for the same RR value, the ratio of ⟨Chl(λ)⟩ to Chl(0.5) also varies widely. For instance, for RR = 0.0, ⟨Chl⟩ to Chl(0.5) varies in a range of ∼1.6−3.1 for the various ways of getting ⟨Chl⟩. These results further highlight the complexity and effect of calculating weighted average of Chl, and the importance of using the same wavelength and the same scheme to get such an average for consistency.

2. Relationship Between R_{rs} and ⟨Chl⟩

For empirical algorithms like Eq. (16), the values of α_{0-4} are determined by a least-square-fit between RR and Chl, with the values of α_{0-4} strictly depending on RR and Chl to be used for the development of such empirical algorithms (see Tables 2 and 7 of [8]). With a data-driven approach, different from Andre [47] and Sokoletsky and Yacobi [32], we evaluated the relationship between RR and the various Chl of this synthetic dataset, including Chl(0.5), $\langle Chl(490)\rangle_{GC\text{ or }Z}$, and $\langle Chl(Kpar)\rangle_{GC\text{ or }Z}$.

Figure 6(a) shows the scatterplots (in log scale) between RR and various Chl of this dataset of highly stratified waters. Following the same fourth-order polynomial scheme for each RR-Chl pair, it is found that the coefficient of determination

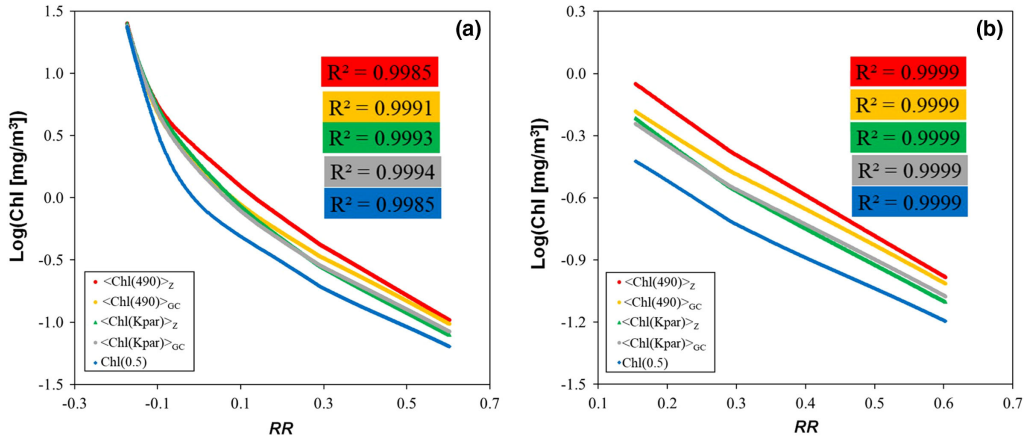

Fig. 6. Example relationships between Chl and RR (band ratio of R_{rs}) for the 1000 cases of stratified waters showing in Fig. 5. (a) for the entire range, while (b) for Chl(0.5) less than 2.0 mg/m^3.

Table 1. Algorithms Coefficients of the Synthetic Dataset and Statistics for the Various Chl Following the OC4 Empirical Scheme

	Coefficient							
	α_0	α_1	α_2	α_3	α_4	R^2	RMSE	bias
$\langle Chl(440)\rangle_Z$	0.2381	−3.7351	9.9516	−22.172	17.35	0.9984	0.0240	-1.4×10^{-5}
$\langle Chl(440)\rangle_{GC}$	0.1459	−3.9053	11.112	−23.652	17.812	0.9989	0.0196	-7.4×10^{-5}
$\langle Chl(490)\rangle_Z$	0.3591	−3.5357	7.7118	−17.814	14.547	0.9985	0.0238	-5.4×10^{-5}
$\langle Chl(490)\rangle_{GC}$	0.2294	−3.8194	9.7772	−20.553	15.417	0.9991	0.0185	-3.0×10^{-7}
$\langle Chl(550)\rangle_Z$	0.4267	−3.9657	5.2424	−8.642	6.7243	0.9990	0.0212	-1.3×10^{-5}
$\langle Chl(550)\rangle_{GC}$	0.3054	−4.0437	7.7888	−14.517	10.676	0.9993	0.0170	-5.7×10^{-6}
$\langle Chl(Kpar)\rangle_Z$	0.2641	−4.1575	8.6008	−16.007	11.702	0.9993	0.0170	-6.8×10^{-6}
$\langle Chl(Kpar)\rangle_{GC}$	0.2055	−4.0903	9.8984	−19.444	14.186	0.9994	0.0161	-9.3×10^{-6}
Chl(0.5)	−0.0399	−4.2128	14.615	−34.631	28.132	0.9985	0.0250	3.4×10^{-5}

(R^2) of the RR-Chl pair is very high (four significant digits are used to highlight the similarity in R^2 values) among the various pairs analyzed, with the R^2 values generally greater than 0.99. Following the scheme of Eq. (16a), empirical algorithms using fourth-order polynomials for each Chl could be developed for such a synthetic dataset, with algorithm coefficients, R^2, root-mean-square error (RMSE) and bias presented in Table 1. Where the RMSE is defined as follows:

$$\mathrm{RMSE}=\sqrt{\frac{\sum_{i=1}^{N}\left(\mathrm{Log}(\langle \mathrm{Chl}\rangle \text{ or } \mathrm{Chl}(0.5))-\mathrm{Log}(\mathrm{Chl}^{\mathrm{RS}})\right)^2}{N}}, \tag{19}$$

and bias is calculated as follows:

$$\mathrm{bias}=\frac{1}{N}\sum_{i=1}^{N}\left(\mathrm{Log}(\langle \mathrm{Chl}\rangle \text{ or } \mathrm{Chl}(0.5))-\mathrm{Log}(\mathrm{Chl}^{\mathrm{RS}})\right). \tag{20}$$

N is the number of samples.

It is found that, although it is a dataset of strong stratifications, R^2 values of all relationships exceeded 0.99, whereas the values of RMSE and bias are practically zero. These results indicate that RR has the same predictability (measured by R^2, RMSE, and bias) for Chl(0.5) compared with the various $\langle$Chl$\rangle$. Further, if the focus is ocean waters (by limiting surface Chl less than 2.0 mg m^{-3}), again, all RR-Chl relationships show nearly identical R^2 values and effectively zero in RMSE and bias (results omitted here). Sokoletsky and Yacobi [32] compared the relationships among the various $\langle$Chl$\rangle$ for measurements in Lake Kinneret, Israel, where the range of Chl is ∼2−400 mg/m^3, and obtained R^2 values greater than 0.96 between Chl(0-1) and $\langle$Chl(Kpar)$\rangle$ for bloom and no-bloom waters. These results are

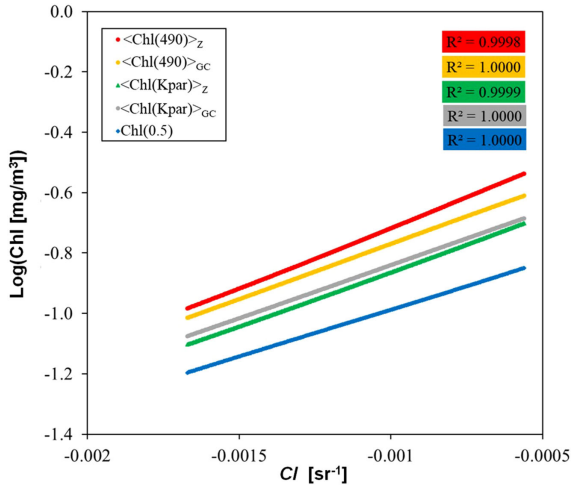

Fig. 7. As Fig. 6, but between Chl and CI (band difference of R_{rs}) and limiting Chl(0.5) less than 0.25 mg/m^3.

Table 2. As Table 1, but for the Band Difference Algorithm

	Coefficient				
	β_0	β_1	R^2	RMSE	bias
$\langle \mathrm{Chl}(440)\rangle_Z$	−0.3886	365.25	1	0.0006	1.7×10^{-7}
$\langle \mathrm{Chl}(440)\rangle_{GC}$	−0.464	339.13	1	0.0006	-2.5×10^{-5}
$\langle \mathrm{Chl}(490)\rangle_Z$	−0.3134	403.44	0.9998	0.0016	-2.9×10^{-5}
$\langle \mathrm{Chl}(490)\rangle_{GC}$	−0.4045	365.44	1	0.0003	-3.5×10^{-5}
$\langle \mathrm{Chl}(550)\rangle_Z$	−0.4295	397.64	0.9996	0.0025	2.0×10^{-5}
$\langle \mathrm{Chl}(550)\rangle_{GC}$	−0.4608	381.9	0.9999	0.0014	-4.8×10^{-5}
$\langle \mathrm{Chl(Kpar)}\rangle_Z$	−0.5011	361.73	0.9999	0.0012	4.1×10^{-5}
$\langle \mathrm{Chl(Kpar)}\rangle_{GC}$	−0.4876	352.29	1	0.0003	3.3×10^{-5}
Chl(0.5)	−0.6769	310.46	1	0.0004	5.2×10^{-6}

generally consistent with the observations here, although we focused on the relationship between RR and ⟨Chl⟩.

Similarly, Fig. 7 shows relationships between the color index (CI) [11] and Chl(0.5) as well as the various ⟨Chl⟩. It is found again that (see Table 2) the predictability of Chl(0.5) is almost the same as that of ⟨Chl⟩ when CI is the input. Note that the algorithm coefficients (α_{0-4}, β_{0-1}) shown in Tables 1 and 2 are not intended for applications with satellite-measured ocean color, as the synthetic data do not necessarily match natural variations. They simply indicate that different sets of algorithm coefficients will be generated when a different Chl is used for the development of such empirical algorithms.

3. Selecting Chl for Empirical Ocean Color Algorithms

Based on the observed small differences between $\langle \mathrm{Chl}(520)\rangle_{GC-1.0}$ and Chl^{RS} from the 443–550 empirical algorithm, Andre [47] suggested that generally the Chl of the surface layer represents Chl^{RS} well, as most of the time the DCM of ocean waters does not make a strong contribution to R_{rs} or r_{rs}. This is also due to the fact that (1) the penetration depth of 520 nm is generally shallower than the blue wavelengths for oceanic waters, and (2) the stratification of the *in situ* dataset [22] is mild, where C_m is generally ∼2 times of C_0. From the results shown above, we extend this argument to situations even when the DCM layer does make strong contributions to R_{rs} and to the present empirical algorithms used to process satellite ocean color data. Andre [47] provided a few reasons, and we further emphasize and extend to:

(1) Empirical algorithms for Chl never use one band for the inversion, rather, they use two to four or many spectral bands. As a result, the effect of stratification at various bands could be more or less compensated for in the empirical algorithms. An earlier example was presented in Gordon for the blue-green band ratio of reflectance [25].

(2) For empirical algorithms, the algorithm coefficients [e.g., α_{0-4} in Eq. (16)] depend on the Chl data used to tune the algorithm. Thus, comparing Chl^{RS} with ⟨Chl⟩ for stratified waters [24], because ⟨Chl(λ)⟩ is dependent on both wavelength and the way of weighting, the empirical algorithm(s) should be first tuned with a clearly described ⟨Chl⟩. In data preparation for the development of such algorithms, however, such a weighted average is not always followed, as the required profiles of optical properties are not always available [28,48,50].

(3) Because of the data-driven nature, as shown in Tables 1 and 2, the use of different ⟨Chl(λ)⟩ or Chl(0.5) will simply result in a different set of empirical algorithm coefficients, but the predictability (measured by R^2, RMSE, and bias) among the various Chl are nearly the same. It is inconsistent to compare Chl^{RS} obtained from an empirical algorithm developed for homogeneous waters with ⟨Chl(λ)⟩, regardless of the wavelength or the way of weighting calculation.

(4) If "surface" Chl is selected to develop empirical algorithms and subsequently to evaluate its performance, the advantage is quite obvious because surface Chl is very easy to be collected and is generally available for all field measurements. More importantly, it bypasses the requirement to have profiles of optical properties for the calculation of ⟨Chl⟩, although it is always useful to include measurements of the light field in the upper water column. Therefore, as pointed out in Sathyendranath *et al.* [28], algorithm development and verification using surface Chl is a better choice, as the use of ⟨Chl⟩ could be intractable.

(5) ⟨Chl(λ)⟩, calculated from whatever weighting scheme, cannot be used as the input for the estimation of primary production [51,52] or the study of phytoplankton phenology [18]. For stratified waters, even if it is ⟨Chl(λ)⟩ used to develop an empirical algorithm and then produced from ocean color measurement, it is necessary to convert $\langle \mathrm{Chl}(\lambda)\rangle^{RS}$ to Chl for other applications in oceanography.

It is necessary to point out that in the above analyses, some of the Chl(z) profiles are likely not realistic, and that the vertical variation of Chl in natural environment may not be modeled with just one parameter (C). For data from natural environment, due to some randomness in the vertical distributions of constituents, as shown in Odermatt *et al.* [30], the R^2 values between RR and Chl will be much lower than 0.99. However, a key assumption for empirical Chl algorithms is that the variation of optical properties are driven by Chl alone. For the natural environment, there are other constituents, e.g., gelbstoff or yellow substance, and their optical properties likely vary independently from Chl; thus, large errors will be introduced to Chl^{RS} empirically derived from RR, stratified or not. Thus, for realistic data, lower R^2 values are expected between RR (or CI)

and ⟨Chl⟩, and between RR (or CI) and Chl(0.5), no matter if the water is homogeneous or not. As indicated in Andre [47], such a lower value in R^2 should not affect the conclusion that the predictability of "surface" Chl will be similar (if not better) than those of ⟨Chl⟩ [32] when empirical algorithms are used for the estimation, stratified or not. For analytical or semi-analytical inversion algorithms, however, the relationships between inverted Chl or IOPs and their vertical profiles are much more complex [35].

5. SUMMARY AND CONCLUSIONS

Because visible light can penetrate to a deeper depth in the upper water column, stratified waters add significant complexity and challenge to the modeling of the subsurface reflectance and the remote sensing of Chl from the measurement of ocean color. There have been studies on both fronts in the past decades, which resulted in models for reflectance using ⟨Chl⟩ or ⟨u⟩ of equivalent homogeneous waters as the input, and suggestions of some kind of ⟨Chl⟩ to compare with Chl^{RS} estimated empirically from R_{rs}. However, there have been limited evaluations of the forward models as well as the applicability of ⟨Chl⟩ for empirically derived Chl^{RS}. In particular, it is not clear which vertical weighting parameter is more appropriate for the calculation of ⟨Chl⟩ or ⟨u⟩; also, it is not certain which ⟨Chl⟩, or whether it is necessary to use ⟨Chl⟩, is needed for the development (and subsequent evaluation) of empirical algorithms for Chl. In this work, using numerically simulated data of stratified waters, we examined the forward models for reflectance and the inverse empirical algorithms for Chl. In particular, the simulations focused on situations that the profiles of the total absorption and backscattering coefficients co-vary with Chl(z), as there will be no "equivalent" homogeneous waters with ⟨Chl⟩ as the concentration if the profiles of the absorption and backscattering coefficients vary independently with Chl(z).

From analyses of the simulated data, it is found that, for the forward model,

1. If using ⟨Chl⟩ of equivalent homogeneous water as the input to estimate r_{rs}, the weighting model of calculating ⟨Chl⟩ proposed by Gordon and Clark [24] and Gordon [25] works well, although depending on the contribution of gelbstoff, the resultant r_{rs} may have errors higher than 10%. Further, the attenuation coefficient of upward light from a depth (κ) required for the model is better assumed as 1.5 times of K_d, rather the default 1.0 times K_d as indicated in Gordon and Clark [24]. The weighting model derived in Zaneveld *et al.* [26] is not appropriate for the calculation of ⟨Chl⟩ to be used to estimate r_{rs} of stratified waters.
2. If using ⟨u⟩ of equivalent homogeneous water as the input to estimate r_{rs}, the weighting model of calculating ⟨u⟩ proposed by Zaneveld *et al.* [26] worked very well. For the calculation of the weighting from a depth, however, it appears that assuming κ as 1.0 times K_d has less errors than assuming κ as 1.5 times K_d. In view of the different weighting formula, the weighting model for ⟨Chl⟩ proposed in Gordon and Clark [24] and Gordon [25] is not appropriate for the calculation of ⟨u⟩, if this ⟨u⟩ is to be used to model r_{rs}.

For the empirical algorithms of estimating Chl from ocean color, or the inverse model, it is found that,

1. As indicated earlier, ⟨Chl(λ)⟩ is not only wavelength dependent, but also weighting-formula dependent. Such a complexity makes it difficult to track the exact nature of ⟨Chl(λ)⟩ when a dataset was prepared; without such details, there will be ambiguities regarding the reported ⟨Chl⟩ values.
2. For stratified waters, although the layer of chlorophyll maximum could contribute to R_{rs}, as long as all optical properties co-vary with Chl(z), a prerequisite for "Case 1" waters, the predictability of surface Chl from RR (or CI) is nearly the same as that of ⟨Chl(λ)⟩. This indicates that, due to the data-driven nature of empirical algorithms and that such simple empirical algorithms are for "Case 1" waters only, it is valid, certainly straightforward, and unambiguous to use Chl of "surface layer" [e.g., Chl(0.5)] for the development of such algorithms. Further, because ⟨Chl(λ)⟩ is complex and difficult to track, it is recommended to avoid the use of ⟨Chl(λ)⟩ for empirical Chl algorithms from ocean color.
3. The empirical coefficients of the present OC4 or CI algorithms were based on a mix of surface Chl and $\langle \text{Chl}(490) \rangle_{\text{GC}-1.0}$ [48], it is expected that a different set of coefficients could result if it is just "surface" Chl used for the development of such empirical algorithms.

APPENDIX A: KEY BIO-OPTICAL RELATIONSHIPS USED IN HYDROLIGHT SIMULATIONS

In addition to the boundary conditions (e.g., radiation from the sun and sky, wind condition, etc.), it is required to know the absorption and scattering coefficients of the water column in order to simulate the light field in water through Hydrolight [31]. Following the conventional practices, the absorption coefficient (a) of the bulk water is modeled as [53,54] follows:

$$a(\lambda) = a_w(\lambda) + a_p(\lambda) + a_g(\lambda). \tag{A1}$$

Values of $a_w(\lambda)$ represent the absorption coefficient of pure seawater, which is available from the literature [55,56]. $a_p(\lambda)$ and $a_g(\lambda)$ are the spectral absorption coefficient of particulate matter and colored dissolved organic matter (CDOM), respectively. For a stratified water column having Chl(z), they are modeled as follows:

$$a_p(z, \lambda) = 0.06 * a_c^*(\lambda)(\text{Chl}(z))^{0.65}, \tag{A2}$$

and

$$a_g(z, \lambda) = a_g(z, 440)\exp^{-0.014(\lambda-440)}. \tag{A3}$$

Values of $a_c{}^*(\lambda)$ are empirical parameters to model the chlorophyll-specific absorption coefficient at λ [57].

The scattering coefficient is modeled as [43] follows:

$$b(\lambda) = b_w(\lambda) + b_p(\lambda), \tag{A4}$$

with values of $b_w(\lambda)$ from the literature [58]. For stratified water having Chl(z), $b_p(z, \lambda)$ is modeled as follows [43]:

$$b_p(z,\lambda) = 0.3(\mathrm{Chl}(z))^{0.6}\left(\frac{550}{\lambda}\right). \quad \textbf{(A5)}$$

The particle scattering phase function is the "Petzold-average" as defined in Mobley [53], with a backscattering ratio of 1.83%, and this phase function is kept the same vertically.

With the previously mentioned setups, both $a_p(z,\lambda)$ and $b_{bp}(z,\lambda)$ co-vary with Chl(z) as indicated in Gordon [25]. Along with the design for $a_g(\lambda)$, $a(z,\lambda)$ also co-varies with Chl(z). For the simulations, the water column is set as infinitely deep; Raman scattering and fluorescence a re e xcluded. The sky is set as cloudless with a sun zenith angle of 30°, and a wind speed of 5 m s^{-1} is used.

Funding. Key Technologies Research and Development Program (2016YFC1400904); National Natural Science Foundation of China (41830102, 41890803, 41941008); The Joint Polar Satellite System (JPSS) funding for the National Oceanic and Atmospheric Administration Color Calibration and Validation (Cal/Val) Project.

Acknowledgment. The National Satellite Ocean Application Service (NSOAS) of China and the University of Massachusetts Boston are greatly appreciated. Comments and suggestions from anonymous reviewers also greatly helped this manuscript.

Disclosures. The authors declare that they have no known competing financial i nterests o r p ersonal r elationships that could have appeared to influence t he w ork r eported i n this paper.

REFERENCES

1. H. R. Gordon, O. B. Brown, and M. M. Jacobs, "Computed relationship between the inherent and apparent optical properties of a flat homogeneous ocean," Appl. Opt. **14**, 417–427 (1975).
2. J. R. V. Zaneveld, "Remote sensed reflectance and its dependence on vertical structure: a theoretical derivation," Appl. Opt. **21**, 4146–4150 (1982).
3. H. R. Gordon, O. B. Brown, R. H. Evans, J. W. Brown, R. C. Smith, K. S. Baker, and D. K. Clark, "A semianalytic radiance model of ocean color," J. Geophys. Res. **93**, 10909–10924 (1988).
4. A. Morel and B. Gentili, "Diffuse reflectance of oceanic waters: its dependence on sun angle as influenced by the molecular scattering contribution," Appl. Opt. **30**, 4427–4438 (1991).
5. S. Sathyendranath and T. Platt, "Analytic model of ocean color," Appl. Opt. **36**, 2620–2629 (1997).
6. Z. P. Lee, K. L. Carder, C. D. Mobley, R. G. Steward, and J. S. Patch, "Hyperspectral remote sensing for shallow waters: 2. Deriving bottom depths and water properties by optimization," Appl. Opt. **38**, 3831–3843 (1999).
7. A. Albert and C. D. Mobley, "An analytical model for subsurface irradiance and remote sensing reflectance in deep and shallow case-2 waters," Opt. Express **11**, 2873–2890 (2003).
8. J. O'Reilly, S. Maritorena, B. G. Mitchell, D. Siegel, K. L. Carder, S. Garver, M. Kahru, and C. McClain, "Ocean color chlorophyll algorithms for SeaWiFS," J. Geophys. Res. **103**, 24937–24953 (1998).
9. K. L. Carder, F. R. Chen, Z. P. Lee, S. K. Hawes, and D. Kamykowski, "Semianalytic moderate-resolution imaging spectrometer algorithms for chlorophyll-a and absorption with bio-optical domains based on nitrate-depletion temperatures," J. Geophys. Res. **104**, 5403–5421 (1999).
10. S. Maritorena, D. A. Siegel, and A. R. Peterson, "Optimization of a semianalytical ocean color model for global-scale applications," Appl. Opt. **41**, 2705–2714 (2002).
11. C. Hu, Z. Lee, and B. Franz, "Chlorophyll a algorithms for oligotrophic oceans: a novel approach based on three-band reflectance difference," J. Geophys. Res. **117**, C01011 (2012).
12. S. Shang, Z.-P. Lee, G. Lin, Y. Li, and X. Li, "Progressive scheme for blending empirical ocean color retrievals of absorption coefficient and chlorophyll concentration from open oceans to highly turbid waters," Appl. Opt. **58**, 3360–3369 (2019).
13. IOCCG, "Remote sensing of inherent optical properties: fundamentals, tests of algorithms, and applications," in *Reports of the International Ocean-Colour Coordinating Group, No. 5*, Z.-P. Lee, ed. (IOCCG, Dartmouth, 2006), p. 126.
14. R. Garcia, Z.-P. Lee, and E. J. Hochberg, "Hyperspectral shallow-water remote sensing with an enhanced benthic classifier," Remote Sens. **10**, 147 (2018).
15. C. R. McClain, S. R. Signorini, and J. R. Christian, "Subtropical gyre variability observedby ocean-color satellittes," Deep-Sea Res. II **51**, 281–301 (2004).
16. M. Kahru and B. G. Mitchell, "Seasonal and nonseasonal variability of satellite-derived chlorophyll and colored dissolved organic matter concentration in the California current," J. Geophys. Res. **106**, 2517–2529 (2001).
17. M. Kahru and B. Mitchell, "Increased phytoplankton blooms detected by ocean color," ASLO Aquatic Sciences Meeting, Nice, France, June, 2009.
18. T. Platt, G. White, III, L. Zhai, S. Sathyendranath, and S. Roy, "The phenology of phytoplankton blooms: ecosystem indicators from remote sensing," Ecol. Model. **220**, 3057–3069 (2009).
19. M. J. Behrenfeld, W. E. Esaias, and K. R. Turpie, "Assessment of primary production at the global scale," in *Phytoplankton productivity. Carbon assimilation in marine and freshwater ecosystems*, P. J. L. Williams, D. N. Thomas, and C. S. Reynolds, eds. (Blackwell Science, 2002), pp. 156–186.
20. S. L. Shang, Q. Dong, Z. P. Lee, Y. Li, Y. S. Xie, and M. J. Behrenfeld, "MODIS observed phytoplankton dynamics in the Taiwan strait: an absorption-based analysis," Biogeosciences **8**, 841–850 (2011).
21. M. R. Lewis, J. J. Cullen, and T. Platt, "Phytoplankton and thermal structure of the upper ocean: consequences of non-uniformity in the chlorophyll profile," J. Geophys. Res. **88**, 2565–2570 (1983).
22. A. Morel and J. F. Berthon, "Surface pigments, algal biomass profiles, and potential production of the euphotic layer: relationships reinvestigated in review of remote-sensing applications," Limnol. Oceanogr. **34**, 1545–1562 (1989).
23. J. J. Cullen, "Subsurface chlorophyll maximum layers: enduring enigma or mystery solved?" Annu. Rev. Mar. Sci. **7**, 207–239 (2015).
24. H. R. Gordon and D. K. Clark, "Remote sensing optical properties of a stratified ocean: an improved interpretation," Appl. Opt. **19**, 3428–3430 (1980).
25. H. R. Gordon, "Diffuse reflectance of the ocean: influence of nonuniform phytoplankton pigment profile," Appl. Opt. **31**, 2116–2129 (1992).
26. J. R. V. Zaneveld, A. H. Barnard, and E. Boss, "Theoretical derivation of the depth average of remotely sensed optical parameters," Opt. Express **13**, 9052–9061 (2005).
27. M. Stramska and D. Stramski, "Effects of a nonuniform vertical profile of chlorophyll concentration on remote-sensing reflectance of the ocean," Appl. Opt. **44**, 1735–1747 (2005).
28. S. Sathyendranath, R. J. W. Brewin, C. Brockmann, V. Brotas, B. Calton, A. Chuprin, P. Cipollini, A. B. Couto, J. Dingle, R. Doerffer, C. Donlon, M. Dowell, A. Farman, M. Grant, S. Groom, A. Horseman, T. Jackson, H. Krasemann, V. Lavender, H. Martinez-Vicente, C. Mazeran, F. Mélin, T. Moore, D. Mueller, P. Regner, S. Roy, C. Steele, F. Steinmetz, J. Swinton, M. Taberner, A. Thompson, A. Valente, M. Zühlke, V. Brando, H. Feng, G. Feldman, B. Franz, R. Frouin, R. Gould, S. B. Hooker, M. Kahru, S. Kratzer, B. G. Mitchell, F. Müller-Karger, H. M. Sosik, K. Voss, J. Werdell, and T. Platt, "An ocean-colour time series for use in climate studies: the experience of the ocean-colour climate change initiative (OC-CCI)," Sensors **19**, 4285 (2019).

29. T. Kutser, L. Metsamaa, and A. G. Dekker, "Influence of the vertical distribution of cyanobacteria in the water column on the remote sensing signal," Estuarine, Coastal Shelf Sci. **78**, 649–654 (2008).
30. D. Odermatt, F. Pomati, J. Pitarch, J. Carpenter, M. Kawka, M. Schaepman, and A. Wüest, "MERIS observations of phytoplankton blooms in a stratified eutrophic lake," Remote Sens. Environ. **126**, 232–239 (2012).
31. C. D. Mobley and L. K. Sundman, *HydroLight 5.2 User's Guide* (Sequoia Scientific, 2013).
32. L. G. Sokoletsky and Y. Z. Yacobi, "Comparison of chlorophyll a concentration detected by remote sensors and other chlorophyll indices in inhomogeneous turbid waters," Appl. Opt. **50**, 5570–5579 (2012).
33. W. D. Philpot, "Radiative transfer in stratified waters: a single-scattering approximation for irradiance," Appl. Opt. **26**, 4123–4132 (1987).
34. H. R. Gordon and W. R. Mcluney, "Estimation of the depth of sunlight penetration in the sea for remote sensing," Appl. Opt. **14**, 413–416 (1975).
35. Z. Lee, S. Shang, Y. Wang, J. Wei, and J. Ishizaka, "Nature of optical products inverted semianalytically from remote sensing reflectance of stratified waters," Limnol. Oceanogr. **65**, 387–400 (2020).
36. J. Piskozub, T. Neumann, and L. Woźniak, "Ocean color remote sensing: choosing the correct depth weighting function," Opt. Express **16**, 14683–14688 (2008).
37. J. T. O. Kirk, "A Monte Carlo study of the nature of the underwater light field in, and the relationships between optical properties of, turbid yellow waters," Aust. J. Mar. Freshwater Res. **32**, 517–532 (1981).
38. T. Platt and S. Sathyendranath, "Oceanic primary production: estimation by remote sensing at local and regional scales," Science **241**, 1613–1620 (1988).
39. C. D. Mobley, "Estimation of the remote-sensing reflectance from above-surface measurements," Appl. Opt. **38**, 7442–7455 (1999).
40. Z. P. Lee, K. P. Du, and R. Arnone, "A model for the diffuse attenuation coefficient of downwelling irradiance," J. Geophys. Res. **110**, C02016 (2005).
41. Z. P. Lee, K. L. Carder, and R. Arnone, "Deriving inherent optical properties from water color: A multi-band quasi-analytical algorithm for optically deep waters," Appl. Opt. **41**, 5755–5772 (2002).
42. R. C. Smith, "Remote sensing and depth distribution of ocean chlorophyll," Mar. Ecol. Prog. Ser. **5**, 359–362 (1981).
43. H. R. Gordon and A. Morel, *Remote Assessment of Ocean Color for Interpretation of Satellite Visible Imagery: A Review* (Springer-Verlag, 1983).
44. S. Sathyendranath and T. Platt, "Remote sensing of ocean chlorophyll: consequence of nonuniform pigment profile," Appl. Opt. **28**, 490–495 (1989).
45. Z. P. Lee, C. Hu, S. Shang, K. Du, M. Lewis, R. Arnone, and R. Brewin, "Penetration of UV-Visible solar light in the global oceans: Insights from ocean color remote sensing," J. Geophys. Res. **118**, 4241–4255 (2013).
46. P. J. Werdell, C. S. Roesler, and J. I. Goes, "Discrimination of phytoplankton functional groups using an ocean reflectance inversion model," Appl. Opt. **53**, 4833–4849 (2014).
47. J. M. Andre, "Ocean color remote-sensing and the subsurface vertical structure of phytoplankton pigments," Deep-Sea Res. **39**, 763–779 (1992).
48. P. J. Werdell and S. W. Bailey, "An improved bio-optical data set for ocean color algorithm development and satellite data product validation," Remote Sens. Environ. **98**, 122–140 (2005).
49. A. Morel, "Optical modeling of the upper ocean in relation to its biogenous matter content (Case I waters)," J. Geophys. Res. **93**, 10749–10768 (1988).
50. A. Valente, S. Sathyendranath, V. Brotas, S. Groom, M. Grant, M. Taberner, D. Antoine, R. Arnone, W. M. Balch, K. Barker, R. Barlow, S. Bélanger, J.-F. Berthon, S. Besiktepe, V. Brando, E. Canuti, F. Chavez, H. Claustre, R. Crout, R. Frouin, C. García-Soto, T. W. Gibb, R. Gould, S. Hooker, M. Kahru, H. Klein, S. Kratzer, H. Loisel, D. McKee, B. G. Mitchell, T. Moisan, F. Muller-Karger, L. O'Dowd, M. Ondrusek, A. J. Poulton, M. Repecaud, T. Smyth, H. M. Sosik, M. Twardowski, K. Voss, J. Werdell, M. Wernand, and G. Zibordi, "A compilation of global bio-optical in situ data for ocean-colour satellite applications," Earth Syst. Sci. Data **8**, 235–252 (2016).
51. K. Arrigo, D. Worthen, A. Schnell, and M. P. Lizotte, "Primary production in Southern Ocean waters," J. Geophys. Res. **103**, 15587–15600 (1998).
52. M. J. Behrenfeld and P. G. Falkowski, "A consumer's guide to phytoplankton primary productivity models," Limnol. Oceanogr. **42**, 1479–1491 (1997).
53. C. D. Mobley, *Light and Water: radiative transfer in natural waters* (Academic, 1994).
54. A. Morel and S. Maritorena, "Bio-optical properties of oceanic waters: a reappraisal," J. Geophys. Res. **106**, 7163–7180 (2001).
55. Z. Lee, J. Wei, K. Voss, M. Lewis, A. Bricaud, and Y. Huot, "Hyperspectral absorption coefficient of "pure" seawater in the range of 350–550 nm inverted from remote sensing reflectance," Appl. Opt. **54**, 546–558 (2015).
56. J. D. Mason, M. T. Cone, and E. S. Fry, "Ultraviolet (250–550 nm) absorption spectrum of pure water," Appl. Opt. **55**, 7163–7172 (2016).
57. L. Prieur and S. Sathyendranath, "An optical classification of coastal and oceanic waters based on the specific spectral absorption curves of phytoplankton pigments, dissolved organic matter, and other particulate materials," Limnol. Oceanogr. **26**, 671–689 (1981).
58. X. Zhang, L. Hu, and M.-X. He, "Scattering by pure seawater: Effect of salinity," Opt. Express **17**, 5698–5710 (2009).